water

MDPI

Article

Development of Vitamin B6-Mediated Biochar with Nano Zero-Valent Iron Coating for Oxytetracycline Removal through Adsorption and Degradation under Harsh Acidic Conditions

Yuelin Xin [1], Peng Zhang [2,*], Jian Shen [2] and Shaojie Ren [1]

[1] School of Environmental Science and Engineering, Shandong University, Qingdao 266237, China
[2] Institute for Energy, Environment and Sustainable Communities, University of Regina, Regina, SK S4S 0A2, Canada
* Correspondence: pengzhang83@outlook.com

Abstract: Oxytetracycline-containing wastewater, particularly produced by pharmaceutical industries, is too acidic to treat with iron-assisted materials. In order to tackle this issue, vitamin B6-mediated biochar with nano zero-valent iron coating (nZVI/B6@BC) was developed. Oxytetracycline (OTC) removal performance of biochar (BC), vitamin B6-coated biochar (B6@BC), nZVI-coated biochar (nZVI@BC), and vitamin B6-mediated biochar with nano zero-valent iron coating (nZVI/B6@BC) were investigated to analyze contributions and mechanisms of adsorption and degradation. Through modification, the adsorption capacity of B6@BC was slightly increased from 81.38 mg/g of BC to 85.64 mg/g. In the removal test, the 5-min OTC removal efficiencies with nZVI@BC and nZVI/B6@BC were 52.25% and 59.05%, yet the BC and B6@BC were limited to 5.61% and 8.54%. The distinct difference may be attributed to the existence of nZVI on biochar strongly improving the reactivity from adsorption to chemical reaction. Moreover, 98.28% of OTC was removed within 60 min in the nZVI/B6@BC suspension. The adsorption of OTC on BC fitted the Freundlich isotherm, Temkin isotherm, and intramolecular diffusion model, whereas that on B6@BC fitted Langmuir isotherm and pseudo-second-order better. Based on HPLC-MS analyses, there were three pathways proposed for OTC degradation in nZVI/B6@BC suspension. nZVI provided active sites on biochar for OTC degradation through oxidization, de-hydroxylation, ring-opening, reduction, addition, demethylation, and alkylation reactions. B6 as a mediate helped improve the stabilization and distribution of nZVI on biochar, which facilitates the capability of nZVI/B6@BC for OTC removal through adsorption and degradation under acidic conditions. The OTC can not only be captured on biochar but also be metabolized to achieve complete removal from aquatic systems.

Keywords: oxytetracycline; biochar; nZVI; adsorption; degradation; acidic condition

Citation: Xin, Y.; Zhang, P.; Shen, J.; Ren, S. Development of Vitamin B6-Mediated Biochar with Nano Zero-Valent Iron Coating for Oxytetracycline Removal through Adsorption and Degradation under Harsh Acidic Conditions. *Water* **2022**, *14*, 2734. https://doi.org/10.3390/w14172734

Academic Editor: Cidália Botelho

Received: 30 June 2022
Accepted: 29 August 2022
Published: 1 September 2022

1. Introduction

Oxytetracycline (OTC), a broad-spectrum tetracycline antibiotic, is widely used to treat bacterial infections in human beings, livestock, and fish, and OTC release is inevitable during its production and consumption [1]. A large amount of OTC-containing wastewater has been produced from healthcare, agricultural, and industrial sectors worldwide, resulting in severe OTC pollution in aquatic ecosystems [1–5]. In winter, the mean levels of OTC in water and sediment have been reported at 265.35 ng/L and 23.52 ng/g, respectively [6]. Consequently, long-term OTC exposure can not only lead to serious damage to organisms but can also cause resistance gene contamination in the biosphere [7–9]. Therefore, it is desired to develop green and effective technologies to treat OTC wastewater.

Traditional strategies to solve antibiotic pollution include advanced oxidation, filtration, and electrochemistry [3,10,11]. Compared to these, adsorption is a high-efficiency, cost-saving, and environment-friendly technique to remove OTC [12,13]. Recently, biochar materials derived from agricultural wastes through pyrolysis have been investigated to

adsorb OTC [14]. For example, macro-, colloidal- and nano-biochar materials have been examined for OTC adsorption. The colloidal biochar has the highest maximum adsorption capacity of 136.7 mg/g, while the nano one has the lowest value of 113.2 mg/L [15]. Although biochar has a remarkable specific surface area, surface modification studies on biochar have further been investigated to enhance OTC adsorption. Magnetic montmorillonite biochar has maximum OTC adsorption of 58.85 mg/L, which is 2.63 times as large as the original biochar [16]. In addition, vitamin B6 (B6) modification has been undertaken to improve the OTC adsorption of biochar through the increase in hydroxyls on biochar [17]. Additionally, nano zero-valent iron (nZVI) has been composited to biochar to enhance OTC removal through degradation followed by adsorption. Environmental remediation applications of nZVI-BC composites applied to different aspects have shown the reactivity of nZVI composites and oxidative removal capacity of contaminants, such as nitro and chlorinated organics, heavy metals, and antibiotics [18,19]. The OTC adsorption capacity of nZVI-pickling biochar is 196.70 mg/g, and the degradation has also been found through mass spectrometry analysis [20]. The OTC can be partially converted through the Fenton reaction and further degraded to smaller molecules through a ring-opening reaction [21].

However, the pH range of pharmaceutical wastewater is 3.9 to 9.2, which is not suitable for the application of nZVI-biochar, particularly under harsh acidic conditions [22,23]. The coated nZVI would be dissolved and inactivated under such conditions. In addition, OTC has three acid dissociation constants (pKa_1 = 3.30, pKa_2 = 7.68, pKa_3 = 9.69), which can be dissociated to multiple moieties, including tricarbonyl system, phenolic diketone system, and dimethylammonium group under different pH conditions [24–26]. The adsorption capacities of these moieties on biochar would be various due to the electrostatic effect. Although previous studies have focused on OTC adsorption and degradation of iron-modified biochar, there has been no report on such OTC removal under harsh acidic conditions due to the instability of iron. Depending on the pKa = 5.6, vitamin B6 can exist in several different stable forms, which help improve the stability of the material [27]. It provides a solution for developing stable iron-modified biochar. In addition, the mechanisms of adsorption and degradation of OTC moieties in biochar suspension are not clear under harsh acidic conditions. Therefore, as an extension, B6-mediated biochar with nZVI coating (nZVI/B6@BC) is developed to remove OTC through adsorption and degradation under harsh acidic conditions. In detail, the objective of this study entails (1) fabrication of nZVI/B6@BC through liquid-phase reduction, (2) investigation of chemical properties of nZVI/B6@BC through SEM, FTIR, and X-ray analyses, (3) examination of OTC removal performance of nZVI/B6@BC, and (4) exploration of OTC removal mechanism through analyses of adsorption capacities of raw biochar (BC) and B6-coated BC(B6@BC) and degradation pathways in nZVI/B6@BC suspension. The results of this study are expected to help vigorously remove emerging antibiotics through the application of stable modified biochar materials in the real world.

2. Materials and Methods

2.1. Materials

Oxytetracycline Hydrochloride (OTC-HCl $\geq$ 95%) was purchased from Aladdin Chemistry (Shanghai, China). Vitamin B6, $NaBH_4$, and $FeSO_4 \cdot 7H_2O$ were purchased from Sinopharm Chemical Reagent Co., Ltd. (Shanghai, China). These reagents were above analytical grade.

2.2. nZVI/B6@BC Fabrication

Biochar was derived from corn straw particles pyrolyzed at 350 °C for 2 h (filled in a crucible with a lid in a muffle furnace), which was ground and passed through a 200-mesh sieve. The raw biochar was then washed with HCl (0.1 mol/L) to remove acid-soluble impurities at 200 rpm for 2 h at room temperature. Collected biochar was further washed with deionized water repeatedly until the pH of leachate was about neutral. These biochar particles were dried at 60 °C for 12 h (i.e., BC).

The BC (0.5 g) was immersed into the B6 solution (0.25 wt%) and stirred for 24 h at room temperature in the dark. These particles were washed and dried in a vacuum oven at 40 °C for 12 h (i.e., B6@BC). The nZVI/B6@BC was fabricated based on the B6@BC through the liquid-phase reduction method. In detail, the B6@BC was further immersed into 250 mL 0.054 M $FeSO_4$ solution with magnetic stirring, and then 250 mL 0.138 M $NaBH_4$ solution was added by drops [27]. After 30 min reaction, the nZVI could be synthesized according to the following equation:

$$FeSO_4 + 2NaBH_4 + 6H_2O = Fe^0\downarrow + 2B(OH)_3 + 7H_2\uparrow + Na_2SO_4 \quad (1)$$

The collected biochar was washed several times with deionized water and absolute ethanol 3 times, then dried in a vacuum drying oven under 40 °C for 12 h (i.e., nZVI/B6@BC). Then, this nZVI/B6@BC was stored in the centrifugal tube (kept at a low O_2 concentration) for further experiments. The complete preparation process was shown in Figure 1. In order to compare with nZVI/B6@BC, nZVI was also coated on BC to form nZVI-biochar composites (i.e., nZVI@BC) through the aforementioned liquid-phase reduction method.

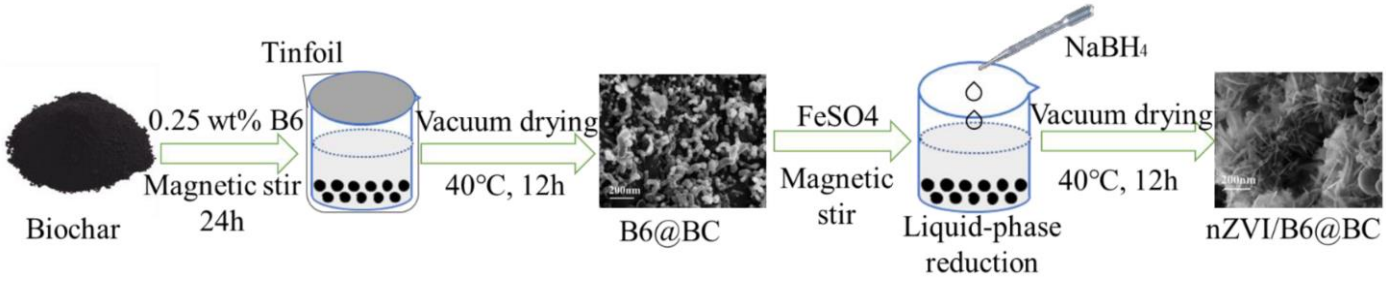

Figure 1. Flow chart of nZVI/B6@BC fabrication.

2.3. Biochar Characterization

Functional groups of nZVI/B6@BC were analyzed by a Fourier transform infrared spectroscope (EQUINOX55, Bruker, Coventry, Germany) with the KBr pellet technique. Surface morphologies of BC, B6@BC, nZVI@BC, and nZVI/B6@BC were observed by scanning electron microscopy (SUPRA55, ZEISS, Heidenheim, Germany). The surface element properties of the nZVI/B6@BC before and after the experiment were acquired by an X-ray photoelectron spectrometer (K-Alpha+, Thermo Scientific, USA) with a source of Al K-alpha.

2.4. OTC Removal Performance

Generally, positively charged ($OTCH_3^+$) and zwitterionic forms ($OTCH_2^{0(+/-)}$) are half/half dominants in OTC solution at a pH level of 3.5. To identify the contributions of adsorption and degradation of nZVI/B6@BC, this pH was chosen in this study. The OTC removal experiment was conducted in multiple 50 mL polyethylene centrifuge tubes containing nZVI/B6@BC-water suspension composed of 500 mg/L OTC and 1.0 g/L nZVI/B6@BC under a pH level of 3.5. These tubes were shaken at 200 rpm at room temperature in the dark. OTC concentrations were analyzed at different times (5 min, 10 min, 15min, 20 min, 30 min, 45 min, 60 min, 90min, 120 min, 360 min, and 720 min), which were measured by HPLC (Thermo Fisher Scientific, Thermo, CA, USA) coupled a UV detector (355 nm) with a C18 column (150 mm × 4.6 mm × 5 μm). The detailed method is described in the SI.

The kinetics were modelled through pseudo-first order and pseudo-second order models, and their coefficients were estimated for analyzing the removal mechanism of OTC in nZVI/B6@BC suspension.

2.5. OTC Adsorption on BC and B6@BC

OTC adsorption on BC and B6@BC was undertaken to investigate adsorption contribution and mechanism in terms of non-degradation assumption on biochar without nZVI.

Different initial OTC concentrations from 100 mg/L to 500 mg/L were carried out until they reached the adsorption balance with 1.0 g/L BC or B6@BC. All experiments were conducted in the dark at 25 °C with pH = 3.5. In addition, adsorption kinetics were also conducted at different time intervals (5 min, 10 min, 15 min, 20 min, 30 min, 45 min, 60 min, 90 min, and 120 min). The adsorption isotherms were fitted by three thermodynamic models: Langmuir isotherm, Freundlich isotherm, and Temkin model, while the kinetics were modelled through pseudo-first-order (a), pseudo-second-order, and intramolecular diffusion models. The model equations fitted in a linear relationship were given in the supporting information. Parallel blank experiments were conducted under the same conditions.

2.6. OTC Degradation Pathway Analysis

Potential degradation pathways of OTC in nZVI/B6@BC suspension were analyzed through HPLC-MS analysis. After the removal tests, degradation products were determined by an HPLC-system (Ultimate 3000, Thermo, Waltham, MA, USA) liquid chromatography with was for OTC and its hydrolysis and degradation products, the column Agilent ZORBAX SB-C18 column (150mm × 4.6mm × 5 μm) column was used to separate OTC and its hydrolysis and degradation products. The mobile phases were acetonitrile (A) and water (formic acid adjusted pH of 2.5, B), flow rate: 0.8 m L/min. High-resolution mass spectrometry (LCQ Fleet, Thermo, Waltham, MA, USA) was equipped with an electrospray ionization source (ESI source). OTC and its hydrolysis and degradation products were identified with positive ion monitoring mode analysis, full scan mode set with a scanning range: 50 to 500 Da, ionization voltage: 4 KV, and capillary temperature: 335 °C. The data of HPLC-MS was analyzed on Thermo Xcalibur.

3. Results and Discussion

3.1. Characterization of Biochar Composite

As shown in Figure 2a, it can be observed that BC has a porous, smooth surface on the fractured layer of biochar with a sharp and flaky structure. Scaled to 200 nm, BC presented a simple and blocky form and had little spatial structure. Compared with BC, Figure 2b shows that the structure of B6-coated biochar had a rough surface, which may indicate that the B6-coating had successfully changed the surface, perhaps because of the B6 adherence to the biochar. The nanoscale nZVI particles observed in Figure 2c indicated that the surface of BC was embedded with nZVI. The aggregation was observed at 500 nm. However, on nZVI/B6@BC, little nZVI aggregation appeared. In Figure 2d, nZVI/B6@BC shows the fine nanosheet structure and small nZVI particle balls, which were well dispersed and attached to B6@BC, indicating that the B6 as an intermediate material can effectively improve the biochar properties as a substrate and provide a wider surface attachment point. The successful B6-layer coating and immobilization of B6@BC tend to reduce the particle size of zero-valent iron particles and the aggregation issue onto unmodified substrates such as raw biochar.

Figure 3 shows the FTIR spectra of BC and nZVI/B6@BC. The differences in the chemical structure of these materials were presented in the range of 400 to 4000 cm^{-1}. Typically, the broad peak around 3430 cm^{-1} was attributed to the O-H [28], and the band around 3550 cm^{-1} was amplified as O-H(free) [29]. The band around 2923 cm^{-1} was assigned to aliphatic hydrocarbon C-H. In addition, the peaks at 1630 cm^{-1} and 1430 cm^{-1} were attributed to C=O vibration (diaryl ketone, quinone, and/or carboxyl groups), while that at 1560 cm^{-1} was aromatic C=C. The band at wavenumber near 1050 cm^{-1} was assigned to the C-OH bending vibration, implying the existence of large numbers of hydroxyl (-OH) and carboxylate (-COOH) groups on the BC. Compared with the original BC, B6@BC decreased the transmittance at 3430 cm^{-1}, indicating that the O-H and N-H bands of B6 succeeded in sticking in the process. In addition, nZVI/B6@BC exhibited that the intensities of the peak at 3430 cm^{-1} and band of 1000 to 1500 cm^{-1} were lower than those of BC due to the deposition of iron on carbon spheres. Besides, the peaks around 800 cm^{-1}, 781 cm^{-1}, and 866 cm^{-1} are intended to be the aromatic C-H [29], illustrating that both the B6-coating and

nZVI attaching processes reduced the amount of aromatic carbon. There were differences between B6@BC and nZVI/B6@BC in peaks at 1035 and 1430, which are supposed to be the C=C, C=O, and C-O bands. These differences indicated the formation of C-O–Fe bonds on nZVI/B6@BC.

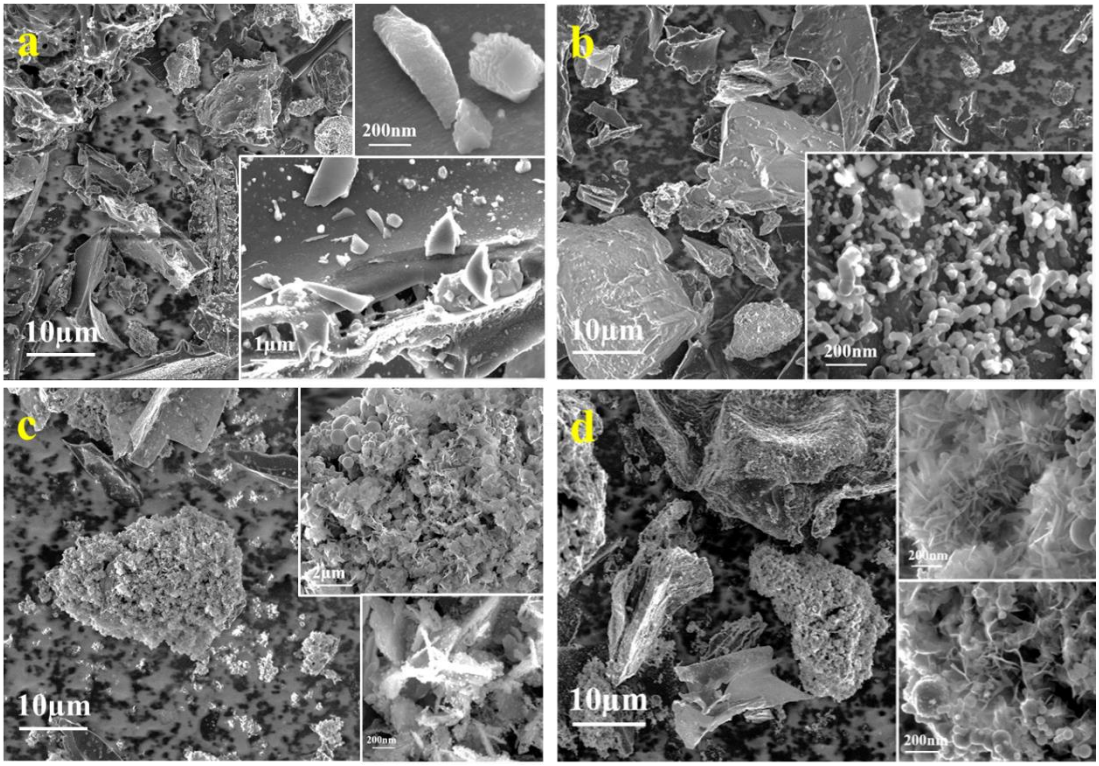

Figure 2. SEM imagines of biochar materials (**a**) BC, (**b**) B6@BC, (**c**) nZVI@BC, and (**d**) nZVI/B6@BC.

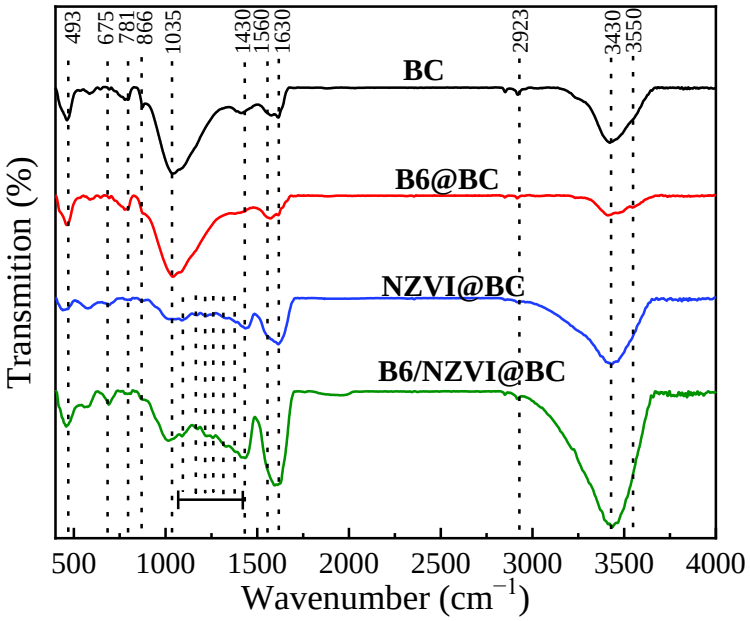

Figure 3. FTIR spectra of biochar materials: BC, B6@BC, nZVI@BC, and nZVI/B6@BC.

Figure 4a shows the XRD patterns of BC, B6@BC, nZVI@BC, and nZVI/B6@BC. For BC and B6@BC, there was a strong peak (2θ = 26.69°) and two small peaks (2θ = 20.77° and 27.79°), which indicated that the amorphous carbon matrix was the main structure. A specific Fe peak at 42.26° was detected obviously in nZVI@BC and nZVI/B6@BC, indicating

the presence of nZVI. In addition, the B6-coating process decreased the intensity of this peak in nZVI/B6@BC. Figure 4b–d show the surface element and high-resolution Fe XPS spectra. Peaks of Fe2*p* were observed in both nZVI@BC and nZVI/B6@BC in Figure 4b. As shown in the high-resolution Fe spectra (Figure 4c,d), there are two dominant peaks of Fe2$p_{1/2}$ and Fe2$p_{3/2}$ in terms of Fe(II) and Fe(III) in both nZVI@BC and nZVI/B6@BC except for Fe^0. In addition, the intensities of Fe(II) and Fe(III) presented more similarity in individual orbitals of nZVI/B6@BC than those of nZVI@BC, which were attributed to improvement in stabilization and distribution of Fe through B6 loading. After the OTC removal experiment, peaks of Fe^0 could hardly be observed in both nZVI@BC and nZVI/B6@BC, while peaks of Fe(II) were increased significantly in these materials. This indicated that Fe reduction was a crucial contribution to OTC degradation.

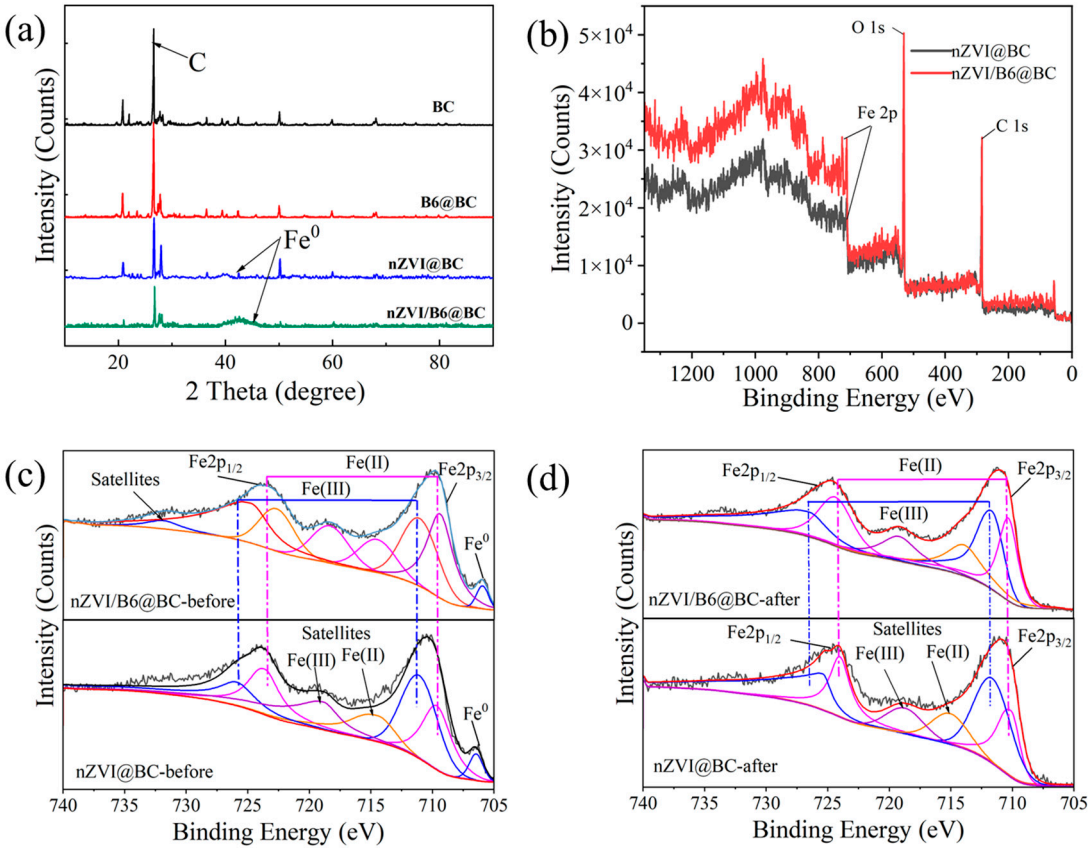

Figure 4. X-ray analyses of biochar materials (**a**) XRD, (**b**) XPS, (**c**) high-resolution Fe spectra of nZVI@BC and nZVI/B6@BC before OTC removal application, and (**d**) high-resolution Fe spectra of nZVI@BC and nZVI/B6@BC after OTC removal application.

3.2. OTC Removal Performance

The removal efficiencies were displayed as the Figure 5 shown in the following order: nZVI/B6@BC > nZVI@BC > B6@BC > BC. The 24-h OTC removal efficiencies in BC and B6@BC suspensions only approached 16.51% and 17.49%, respectively, and no significant change was observed between 2 h and 24 h. It is assumed that there is only adsorption on BC and B6@BC, and the adsorption equilibrium was reached after 2 h. Without the iron modification, the adsorption capacity of B6@BC compared to BC was slightly increased from 81.38 mg/g to 85.64 mg/g only via B6-coating. Meanwhile, the 24-h efficiencies in nZVI/BC and nZVI/B6@BC suspensions approached 98.40% and 98.55%, illustrating that OTC had been almost completely removed. Moreover, the 5-min OTC removal efficiencies in nZVI@BC and nZVI/B6@BC suspensions were 52.25% and 59.05%, respectively. Such dramatically rapid removal rates indicate the great removal performance, which may be due to the strong oxidation of ·OH radicals generated through the Fenton reaction triggered by

iron on biochar. Moreover, 98.28% of OTC was removed within 60 min in the nZVI/B6@BC suspension. It may be attributed to the amino and hydroxyl groups of B6 as a mediate between BC and nZVI, improving the stability of nZVI attachment and generating more active sites on nZVI/B6@BC for OTC removal than nZVI@BC. Furthermore, the reusable performance of nZVI@BC and nZVI/B6@BC were also exanimated through 4-time cycles of OTC removal (Figure S1). Although the removal efficiencies of these two materials declined after multiple cycles, nZVI/B6@BC exhibited a significantly higher removal capacity than nZVI@BC due to the B6-associated stabilization of nZVI.

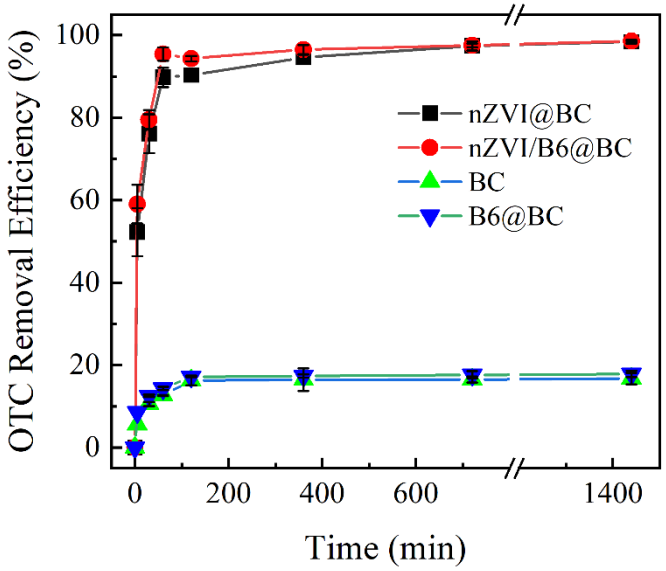

Figure 5. OTC removal performance of biochar materials at 25 °C, pH = 3.5.

3.3. Adsorption Contribution and Mechanism of BC and B6@BC

In order to investigate the assumption that adsorption is the critical effect of BC and B6@BC, modelling analyses were based on the batch OTC adsorption experiments on BC and B6@BC to fitting adsorption isotherm and kinetic processes non-degradation assumption on biochar without nZVI. Figure 6 shows the adsorption isotherms of OTC on BC and B6@BC, while the isotherm parameters are shown in Table S1. B6@BC exhibited a stronger adsorption capacity than BC.

According to the modelling results, the adsorption on BC fitted the Freundlich isotherm (K_f = 11.945 mg/g·(L/mg)$^{1/n}$, n = 2.235, R^2 = 0.9693) and Temkin one (K_T = 0.6747 L/mg, B = 11.158 J/mol, R^2 = 0.9699), while that on B6@BC fitted Langmuir isotherm (Q_m = 52.7869 mg/g, K_l = 0.0349 L/mg, R^2 = 0.9973) better. The heterogenic surface of BC provides diverse surface tension and surface energy which help adsorb OTC [30]. While B6 coating converted to homogenous surface on B6@BC, leading monolayer adsorption on B6@BC. In addition, B6 coating also facilitated OTC physical adsorption through hydrogen bonds and Van der Waals' force [31,32].

On the other hand, the adsorption kinetics are shown in Figure 7, and the kinetic parameters are described in Table S3. The intramolecular diffusion model was the best for BC (K_{int} = 6.0202 mg/(mg·min$^{1/2}$), C = 17.182 mg/g, R^2 = 0.9885), indicating that the adsorption behaviour on the raw biochar mainly depended on physical adsorption. Due to the porous structure of biochar, a long diffusion time was required for OTC to achieve inner adsorption sites to reach saturation. While pseudo-second order was the best model for B6@BC (K_2 = 0.0104 g/(mg·min), Q_e = 90.09 mg/g, R^2 = 0.9928), indicating that there is chemical reaction between B6@BC and OTC. The alkaline pyridine ring of B6 on biochar promoted such a reaction with acidic groups of OTC. In addition, ionic OTC may also facilitate the adsorption on B6-associated hydrophilic biochar. Hence, the

interactions between B6@BC and OTC may be electrostatic interaction, acid–base reaction, and ionic exchange.

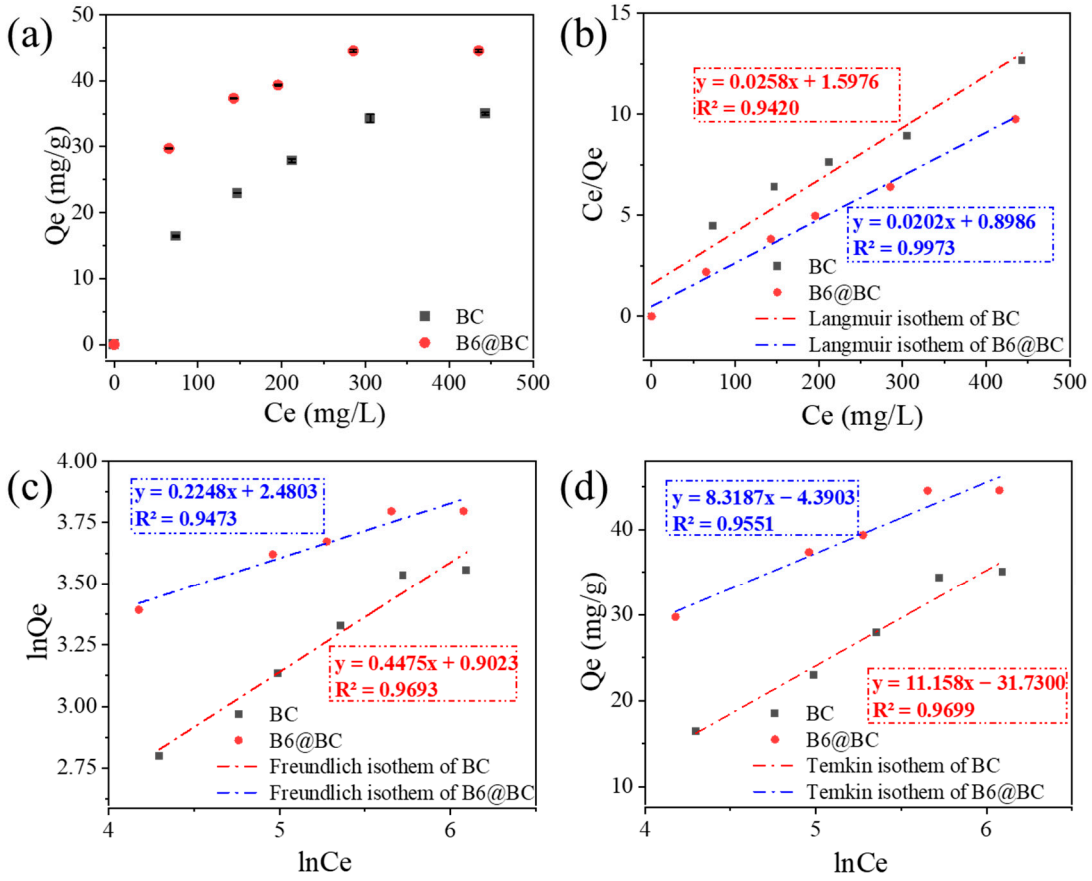

Figure 6. The equilibrium of (**a**) original adsorption capacity and adsorption isotherm modelling (**b**) Langmuir isotherm, (**c**) Freundlich isotherm, and (**d**) Temkin isotherm of OTC on BC and B6@BC.

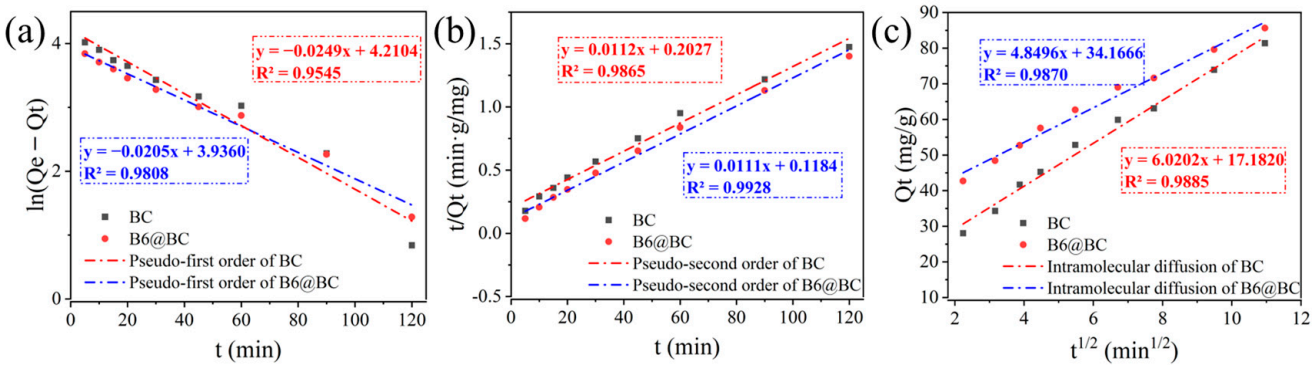

Figure 7. Adsorption kinetic modelling including (**a**) pseudo-first order, (**b**) pseudo-second order, and (**c**) intramolecular diffusion of OTC on BC and B6@BC.

3.4. Degradation Contribution and Mechanism of nZVI@BC and nZVI/B6@BC

According to the kinetic modelling pattern in Figure 8 and the kinetic parameters shown in Table S4, the degradation kinetics of both nZVI@BC and nZVI/B6@BC follow the pseudo-second-order model rather than the pseudo-first-order one, indicating that the chemical reaction between the modified materials and the OTC is the main effect. In addition, there was no significant difference in OTC removal capacities of nZVI@BC and nZVI/B6@BC during 700 min. Meanwhile, the nZVI/B6@BC presented a faster reaction rate

with a larger K_2 than nZVI@BC, which is attributed to better stabilization and distribution of nZVI on biochar through B6 coating.

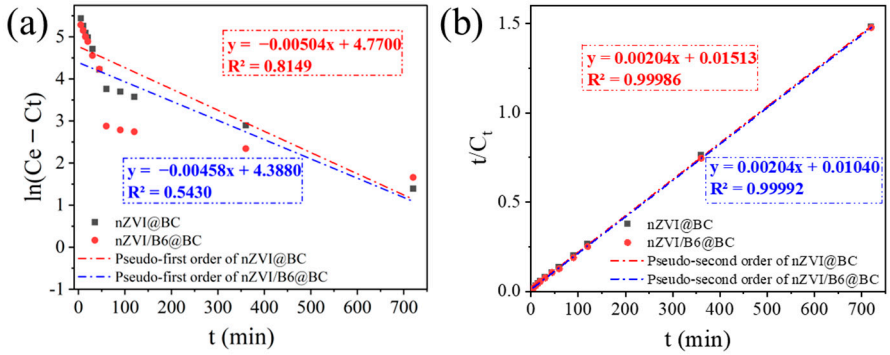

Figure 8. Degradation kinetic modelling (**a**) pseudo-first order, and (**b**) pseudo-second order of OTC on nZVI@BC and nZVI/B6@BC (initial concentration = 500 mg/L, adsorbent concentration = 1.0 g/L, temperature = 25 °C, pH = 3.5).

In this study, OTC was rapidly removed in the first 5 min and showed apparent equilibrium at 120 min. The MS spectra of OTC degradation products are exhibited in Figure S2. The OTC peak sharply decreased or disappeared with the increase in the reaction time in nZVI/B6@BC suspension, and three anions with m/z of 477, 430, and 192 were observed at a relatively high level, which may be the main intermediate products. While dominant ionic fragments were m/z of 460 and 461 (two forms of OTC) in blank, BC, and B6@BC suspensions, indicating that there is not any degradation product in these systems.

Based on the MS spectrum, three pathways of OTC degradation in nZVI/B6@BC suspension are proposed in Figure 9. In pathway A, OTC was metabolized A_1 (m/z 477) and A_2 (m/z 494), corresponding to a previous study [33]. In this pathway, Fe^0 reacted with the O_2 in suspension to generate H_2O_2, as shown in the following equation:

$$Fe^0 + O_2 + 2H^+ = Fe^{2+} + H_2O_2 \quad (2)$$

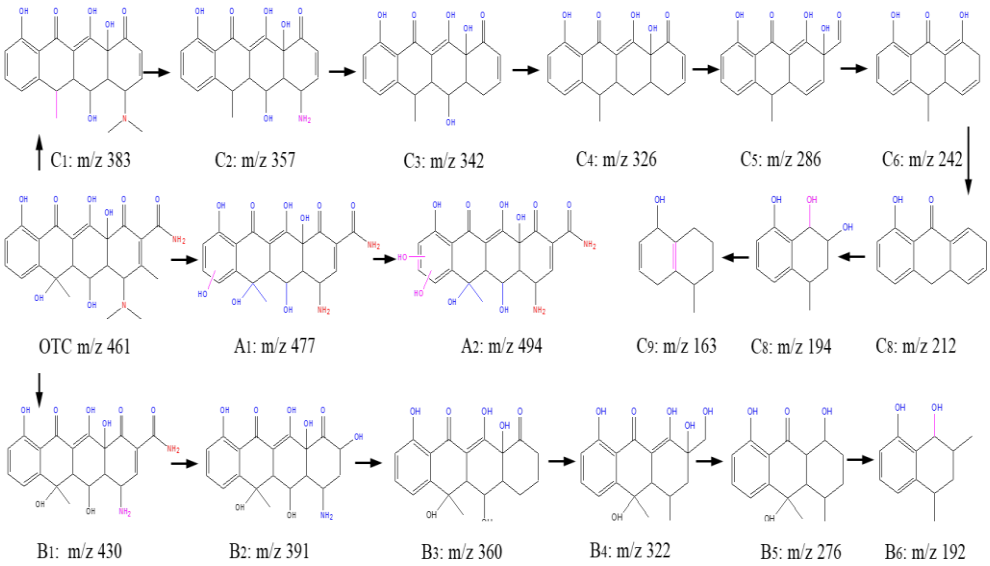

Figure 9. Proposed degradation pathways of OTC in nZVI/B6@BC suspension.

Then, the OH radicals were generated from H_2O_2 and attacked benzene ring on OTC to form phenolic hydroxyl groups, which was similar to the Fenton reaction.

While pathways B and C were opening processes of benzene ring, OTC was metabolized to B_1 (m/z of 430) through conversion of dimethylamine to amine and C_1 (m/z of

383) through loss of hydroxyl, methyl, carboxyl, and amide groups to initialize pathways B and C, respectively [20,33]. On the one hand, B_1 (m/z of 430) converted into B_2 (m/z of 391) and B_3 (m/z of 360) in a two-step reaction of amide loss, followed by a one-step ring-opening reaction, and B_4 (m/z of 322) was generated. Then, hydroxyl groups were detached from the ring to form B_5 (m/z of 276). Finally, the B_6 (m/z of 192) was generated through a ring-opening reaction. On the other hand, the OTC is converted into C_1 (m/z of 383) through the loss of a hydroxyl group and an amide group. C_2 (m/z of 357) was further generated through the conversion of dimethylamine to amine. Consequently, the amine group was off from the carbon ring to form C_3 (m/z of 342). Finally, C_9 (m/z of 163) was produced through multiple reactions, including de-hydroxylation, ring-opening, reduction, addition, demethylation, and alkylation. In nZVI/B6@BC suspension, the OTC was adsorbed on biochar particles, followed by multiple chemical reactions initiated by nZVI on the biochar particles, particularly in acidic conditions.

4. Conclusions

The composite of nZVI/B6@BC was successfully synthesized via liquid-phase coating and reduction reactions. The B6 coating process improved the distribution and stabilization of ZVI nanosheets on biochar due to the mediation of the B6-associated hydrophilic layer between ZVI and biochar. This composite exhibited excellent OTC removal performance through adsorption and degradation. Compared to BC, the adsorption capacity of B6@BC was slightly increased from 81.38 mg/g to 85.64 mg/g through the B6-coating process. In the removal test, the 5-min OTC removal efficiencies in nZVI@BC and nZVI/B6@BC suspensions were 52.25% and 59.05%, while in BC and B6@BC, they were limited to 5.61% and 8.54%. The distinct difference illustrated the existence of nZVI on biochar strongly improving the reactivity of nZVI/B6@BC. Moreover, 98.28% of OTC was removed within 60 min in the nZVI/B6@BC suspension, indicating an excellent removal effect. Through modelling analysis, the adsorption on BC fitted the Freundlich and Temkin isotherms, while that on B6@BC fitted the Langmuir isotherm better. At the same time, the intramolecular diffusion model was the best for BC, while the pseudo-second-order was best fitted on B6@BC. Based on HPLC-MS analyses, there were three pathways proposed for OTC degradation by nZVI/B6@BC. B6 as a mediate helped improve stability and distribution of nZVI on biochar, providing active sites on biochar for OTC degradation through chemical oxidization and reduction, ring-opening, etc., which facilitates nZVI/B6@BC for OTC removal through adsorption and degradation under acidic conditions. The OTC can not only be captured on biochar but also be metabolized to achieve removal from aquatic systems. The degradation products were consistent with the previous literature, which may still be very toxic and require subsequent treatment. The developed nZVI/B6@BC is a modified, high-efficiency and cost-saving material which is expected to be applied to pharmaceutical wastewater treatment.

Supplementary Materials: The following are available online at https://www.mdpi.com/article/10.3390/w14172734/s1. The relevant adsorption isotherm models and kinetic models was referred to the previous articles [17,34]. Figure S1: The removal rate in four cycles OTC exposure experiment by nZVI @BC and nZVI/B6@BC; Figure S2: Dissolution of iron of nZVI/B6@BC and nZVI@BC in acid conditions (pH = 3.5) exposure cycles under a) pure deionized water adjusted by hydrochloric acid and b) 500 mg/L OTC solutions; Figure S3: The HPLC-MS spectra of (a) OTC blank and residues in suspensions of (b) BC after 120 min, (c) B6@BC after 120 min, (d) nZVI@BC after 5 min, (e) nZVI/B6@BC after 5 min, (f) nZVI@BC after 120 min and (g) nZVI/B6@BC after 120 min; Table S1: Zeta potential of different composites in aqueous water; Table S2: The isotherm parameters of oxytetracycline adsorption onto BC and B6@BC at 25 °C and pH = 3.5; Table S3: The kinetic parameters of oxytetracycline adsorption onto BC and B6@BC at 25 °C and pH = 3.5; Table S4: The kinetic parameters of oxytetracycline removal onto nZVI@BC and nZVI/B6@BC at 25 °C and pH = 3.5.

Author Contributions: Investigation, Y.X.; Data curation, Y.X.; methodology, P.Z. & S.R.; validation, P.Z.; formal analysis, Y.X.; writing—original draft preparation, Y.X.; writing—review and editing, P.Z., J.S., & S.R.; visualization, J.S.; supervision, P.Z.; project administration, J.S. All authors have read and agreed to the published version of the manuscript.

Funding: This research received no external funding.

Informed Consent Statement: Not applicable.

Data Availability Statement: The data presented in this study are available on request from the corresponding author. The data are not publicly available due to privacy.

Acknowledgments: We are very grateful for the helpful input from the editor and anonymous reviewers.

Conflicts of Interest: The authors declare no conflict of interest.

References

1. Langbehn, R.K.; Michels, C.; Soares, H.M. Antibiotics in wastewater: From its occurrence to the biological removal by environmentally conscious technologies. *Environ. Pollut.* **2021**, *275*, 116603. [CrossRef] [PubMed]
2. Zhang, Z.H.; Gao, P.; Cheng, J.Q.; Liu, G.H.; Zhang, X.Q.; Feng, Y.J. Enhancing anaerobic digestion and methane production of tetracycline wastewater in EGSB reactor with GAC/NZVI mediator. *Water Res.* **2018**, *136*, 54–63. [CrossRef] [PubMed]
3. Lu, Z.-Y.; Ma, Y.-L.; Zhang, J.-T.; Fan, N.-S.; Huang, B.-C.; Jin, R.-C. A critical review of antibiotic removal strategies: Performance and mechanisms. *J. Water Process Eng.* **2020**, *38*, 101681. [CrossRef]
4. Xue, X.D.; Fang, C.R.; Zhuang, H.F. Adsorption behaviors of the pristine and aged thermoplastic polyurethane microplastics in Cu(II)-OTC coexisting system. *J. Hazard. Mater.* **2021**, *407*, 124835. [CrossRef]
5. Chen, H.; Luo, H.J.; Lan, Y.C.; Dong, T.T.; Hu, B.J.; Wang, Y.P. Removal of tetracycline from aqueous solutions using polyvinylpyrrolidone (PVP-K30) modified nanoscale zero valent iron. *J. Hazard. Mater.* **2011**, *192*, 44–53. [CrossRef] [PubMed]
6. Han, Q.F.; Song, C.; Sun, X.; Zhao, S.; Wang, S.G. Spatiotemporal distribution, source apportionment and combined pollution of antibiotics in natural waters adjacent to mariculture areas in the Laizhou Bay, Bohai Sea. *Chemosphere* **2021**, *279*, 130381. [CrossRef]
7. Liu, G.; Thomsen, L.E.; Olsen, J.E. Antimicrobial-induced horizontal transfer of antimicrobial resistance genes in bacteria: A mini-review. *J. Antimicrob. Chemother.* **2022**, *77*, 556–567. [CrossRef]
8. Lerminiaux, N.A.; Cameron, A.D.S. Horizontal transfer of antibiotic resistance genes in clinical environments. *Can. J. Microbiol.* **2019**, *65*, 34–44. [CrossRef]
9. Qiu, X.W.; Zhou, G.X.; Wang, H.J. Nanoscale zero-valent iron inhibits the horizontal gene transfer of antibiotic resistance genes in chicken manure compost. *J. Hazard. Mater.* **2022**, *422*, 126883. [CrossRef]
10. Yuan, Q.; Zhang, D.; Yu, P.; Sun, R.; Javed, H.; Wu, G.; Alvarez, P.J.J. Selective Adsorption and Photocatalytic Degradation of Extracellular Antibiotic Resistance Genes by Molecularly-Imprinted Graphitic Carbon Nitride. *Environ. Sci. Technol.* **2020**, *54*, 4621–4630. [CrossRef]
11. Zhang, P.; Huang, G.; An, C.; Fu, H.; Gao, P.; Yao, Y.; Chen, X. An integrated gravity-driven ecological bed for wastewater treatment in subtropical regions: Process design, performance analysis, and greenhouse gas emissions assessment. *J. Clean. Prod.* **2019**, *212*, 1143–1153. [CrossRef]
12. Hameed, R.; Lei, C.; Lin, D. Adsorption of organic contaminants on biochar colloids: Effects of pyrolysis temperature and particle size. *Environ. Sci. Pollut. Res. Int.* **2020**, *27*, 18412–18422. [CrossRef]
13. Zhang, H.; Song, X.; Zhang, J.; Liu, Y.; Zhao, H.; Hu, J.; Zhao, J. Performance and mechanism of sycamore flock based biochar in removing oxytetracycline hydrochloride. *Bioresour. Technol.* **2022**, *350*, 126884. [CrossRef]
14. Zhang, P.; Sun, H.; Yu, L.; Sun, T. Adsorption and catalytic hydrolysis of carbaryl and atrazine on pig manure-derived biochars: Impact of structural properties of biochars. *J. Hazard. Mater.* **2013**, *244–245*, 217–224. [CrossRef]
15. Ramanayaka, S.; Kumar, M.; Etampawala, T.; Vithanage, M. Macro, colloidal and nanobiochar for oxytetracycline removal in synthetic hydrolyzed human urine. *Environ. Pollut.* **2020**, *267*, 115683. [CrossRef]
16. Liang, G.; Wang, Z.; Yang, X.; Qin, T.; Xie, X.; Zhao, J.; Li, S. Efficient removal of oxytetracycline from aqueous solution using magnetic montmorillonite-biochar composite prepared by one step pyrolysis. *Sci. Total Environ.* **2019**, *695*, 133800. [CrossRef]
17. Saremi, F.; Miroliaei, M.R.; Shahabi Nejad, M.; Sheibani, H. Adsorption of tetracycline antibiotic from aqueous solutions onto vitamin B6-upgraded biochar derived from date palm leaves. *J. Mol. Liq.* **2020**, *318*, 114126. [CrossRef]
18. Ahmad, S.; Liu, X.; Tang, J.; Zhang, S. Biochar-supported nanosized zero-valent iron (nZVI/BC) composites for removal of nitro and chlorinated contaminants. *Chem. Eng. J.* **2022**, *431*, 133187. [CrossRef]
19. Tarekegn, M.M.; Hiruy, A.M.; Dekebo, A.H. Nano zero valent iron (nZVI) particles for the removal of heavy metals (Cd(2+), Cu(2+) and Pb(2+)) from aqueous solutions. *RSC Adv.* **2021**, *11*, 18539–18551. [CrossRef]
20. Li, Q.; Zhao, S.; Wang, Y. Mechanism of Oxytetracycline Removal by Coconut Shell Biochar Loaded with Nano-Zero-Valent Iron. *Int. J. Environ. Res. Public Health* **2021**, *18*, 13107. [CrossRef]

21. Nguyen, C.H.; Tran, M.L.; Tran, T.T.V.; Juang, R.S. Efficient removal of antibiotic oxytetracycline from water by Fenton-like reactions using reduced graphene oxide-supported bimetallic Pd/nZVI nanocomposites. *J. Taiwan Inst. Chem. Eng.* **2021**, *119*, 80–89. [CrossRef]
22. Wu, Y.W.; Yue, Q.Y.; Gao, Y.; Ren, Z.F.; Gao, B.Y. Performance of bimetallic nanoscale zero-valent iron particles for removal of oxytetracycline. *J. Environ. Sci.-China* **2018**, *69*, 173–182. [CrossRef] [PubMed]
23. Gadipelly, C.; Pérez-González, A.; Yadav, G.D.; Ortiz, I.; Ibáñez, R.; Rathod, V.K.; Marathe, K.V. Pharmaceutical Industry Wastewater: Review of the Technologies for Water Treatment and Reuse. *Ind. Eng. Chem. Res.* **2014**, *53*, 11571–11592. [CrossRef]
24. Xiang, W.; Wan, Y.; Zhang, X.; Tan, Z.; Xia, T.; Zheng, Y.; Gao, B. Adsorption of tetracycline hydrochloride onto ball-milled biochar: Governing factors and mechanisms. *Chemosphere* **2020**, *255*, 127057. [CrossRef]
25. Punamiya, P.; Sarkar, D.; Rakshit, S.; Datta, R. Effectiveness of Aluminum-based Drinking Water Treatment Residuals as a Novel Sorbent to Remove Tetracyclines from Aqueous Medium. *J. Environ. Qual.* **2013**, *42*, 1449–1459. [CrossRef]
26. Leal, J.F.; Santos, E.B.H.; Esteves, V.I. Oxytetracycline in intensive aquaculture: Water quality during and after its administration, environmental fate, toxicity and bacterial resistance. *Rev. Aquac.* **2018**, *11*, 1176–1194. [CrossRef]
27. Radoman, T.S.; Džunuzović, J.V.; Grgur, B.N.; Gvozdenović, M.M.; Jugović, B.Z.; Miličević, D.S.; Džunuzović, E.S. Improvement of the epoxy coating properties by incorporation of polyaniline surface treated TiO 2 nanoparticles previously modified with vitamin B6. *Prog. Org. Coat.* **2016**, *99*, 346–355. [CrossRef]
28. Wang, X.; Lian, W.; Sun, X.; Ma, J.; Ning, P. Immobilization of NZVI in polydopamine surface-modified biochar for adsorption and degradation of tetracycline in aqueous solution. *Front. Environ. Sci. Eng.* **2018**, *12*, 9. [CrossRef]
29. Wang, S.; Zhao, M.; Zhou, M.; Li, Y.C.; Wang, J.; Gao, B.; Sato, S.; Feng, K.; Yin, W.; Igalavithana, A.D.; et al. Biochar-supported nZVI (nZVI/BC) for contaminant removal from soil and water: A critical review. *J. Hazard. Mater.* **2019**, *373*, 820–834. [CrossRef]
30. Liu, W.-J.; Jiang, H.; Yu, H.-Q. Emerging applications of biochar-based materials for energy storage and conversion. *Energy Environ. Sci.* **2019**, *12*, 1751–1779. [CrossRef]
31. Zhang, Y.; Xu, Q.; Sun, M.; Xiong, C.; Wang, P.; Chen, Z.; Sun, G.; Guan, J.; Ding, Z.; Li, M.; et al. Insights into vitamin B3, B6 and C as inhibitor of steel reinforcement: A DFT + U study. *Constr. Build. Mater.* **2021**, *294*, 123571. [CrossRef]
32. Atinafu, D.G.; Jin Chang, S.; Kim, K.-H.; Kim, S. Tuning surface functionality of standard biochars and the resulting uplift capacity of loading/energy storage for organic phase change materials. *Chem. Eng. J.* **2020**, *394*, 125049. [CrossRef]
33. Tran, M.L.; Nguyen, C.H.; Tran, T.T.V.; Juang, R.S. One-pot synthesis of bimetallic Pt/nZVI nanocomposites for enhanced removal of oxytetracycline: Roles of morphology changes and Pt catalysis. *J. Taiwan Inst. Chem. Eng.* **2020**, *111*, 130–140. [CrossRef]
34. Zhang, H.; Wang, J.; Zhou, B.; Zhou, Y.; Dai, Z.; Zhou, Q.; Chriestie, P.; Luo, Y. Enhanced adsorption of oxytetracycline to weathered microplastic polystyrene: Kinetics, isotherms and influencing factors. *Environ. Pollut.* **2018**, *243*, 1550–1557. [CrossRef]